

## *Analysis of the Radiation Characteristics of a Primary-Feed Waveguide in a Quasi-Optical Antenna for Circular $TE_{0n}$ Mode*

Osami WADA\*

(Received October 16, 1989)

### SYNOPSIS

Are calculated the radiation characteristics of two types of primary-feed waveguides of millimeter wave quasi-optical antennas, which transform circular  $TE_{0n}$  mode into a linearly polarized beam. These antennas are utilized for heating and diagnostics of fusion plasma. Analysis is based on the Huygens-Fresnel principle, which takes the diffraction effect into account. For Convenience in analysis, a feed waveguide is divided into two sections, a uniform waveguide section and a visor section. Assuming that the diameter of the waveguide is several times as large as the wavelength and that the structure of the visor is open, the radiation field is approximated by superposition of direct radiation, and first and second reflection on the visor. Numerical results are presented and compared with experimental results. In these types of waveguides, the shadow section on the visor has a great influence on the radiation field. The results of calculation show that the length of the visor should be longer than that obtained by the geometrical optics, and the longer visor reduces the side-lobe level in the direction of the waveguide axis. The results agree well with those in experiments.

---

\* Department of Electrical and Electronic Engineering

## 1. INTRODUCTION

Quasi-optical reflector antennas have been used in heating and diagnostics of fusion plasma. These antennas convert high-power millimeter wave generated by a gyrotron into a linearly polarized beam.<sup>1-3)</sup> The fundamental principle of the antenna is based on the geometrical optics.

The author proposed a method to calculate the radiation characteristics of a few types of the antennas,<sup>3)</sup> each of which consists of a primary feed waveguide and a reflector. The radiation from an antenna is calculated by means of integration of electromagnetic field on a mirror image of a primary source feed, formed by the reflector. Field distribution on the image source is calculated by use of the geometrical-optics approximation, which is valid only in the case that the primary feed waveguide is highly oversized.

In most of practical cases diameters of feed waveguides are, however, not sufficiently large; for example, 37 mm at 28 GHz operation:  $d/\lambda = 3.46$ ,<sup>4)</sup> or 30.0 mm at 60 GHz:  $d/\lambda = 6.00$ ,<sup>5)</sup> where  $d$  denotes a diameter of the waveguide and  $\lambda$  denotes the wavelength. Consequently the size and shape of the waveguide aperture affects the radiation characteristics. In other words, one can calculate the direction of the main lobe and the width of it by the geometrical-optics approximation, but cannot estimate side-lobe level or the efficiency of power transformation accurately for lack of consideration of diffraction effect at the primary feed.

In this paper I will discuss the radiation characteristics of two types of primary-feed waveguides shown in Fig. 1. Analysis is based on the Huygens-Fresnel principle, which takes the diffraction effect into account. A feed waveguide is divided into two sections as shown in Fig. 2, an uniform waveguide section and a visor section. Field is radiated from the waveguide section and reflected on the visor section. Some portion of the field is repeatedly reflected on

the visor. But higher-order reflection field is sufficiently small, assuming that the diameter of the waveguide is several times as large as the wavelength and that the structure of the visor is open. In this paper therefore it is assumed that the radiation field is approximately represented by superposition of direct radiation, and first and second reflection on the visor. In order to simplify the calculation of total radiation field, we will introduce a virtual surface  $S_A + S_B$  as shown in Fig. 2. In the first stage of calculation, field on the virtual surface is calculated, and in the second stage total radiation from the feed is calculated in integration of the field on the surface  $S_A + S_B$ . Some numerical results will also be presented and compared with experimental results.



(a) Stair-cut feed. (b) Oblique-cut feed.

Fig. 1 Primary-feed waveguides of quasi-optical antennas for circular  $TE_{0n}$  mode.

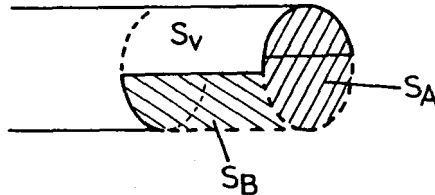


Fig. 2 A visor and virtual aperture used in the present analysis.

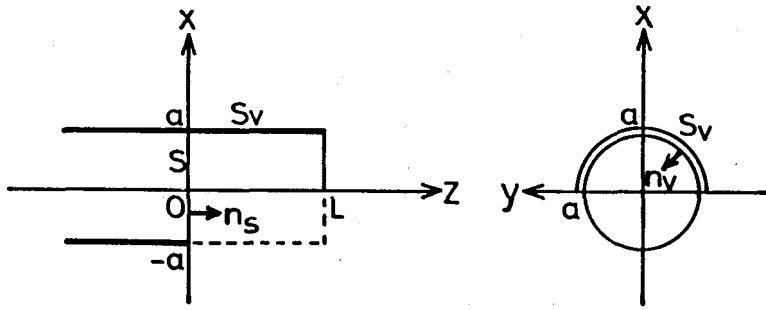


Fig. 3 The system of coordinates and dimensions of a waveguide feed.

## 2. FORMULATION

In order to calculate radiation field from a feed waveguide shown in Fig. 1(a), we consider a coordinate system on an aperture of a circular waveguide as shown in Fig. 3. Let the circular aperture at  $z = 0$  be  $S$ , whose radius is  $a$ , and the surface of the visor section be  $S_v$ . Unit normal vectors on the two surfaces are denoted by  $n_s$  and  $n_v$  respectively.

Assuming discontinuity of the waveguide at  $z = 0$  is negligible, the radiation field from the surface  $S$  is obtained by integration of electromagnetic field on  $S$  as follows.

$$E_i = \int_S \{-j\omega\mu(n_s \times H_s)g + (n_s \times E_s) \times \nabla g + (n_s \cdot E_s) \nabla g\} dS \quad (1a)$$

$$H_i = \int_S \{j\omega\varepsilon(n_s \times E_s)g + (n_s \times H_s) \times \nabla g + (n_s \cdot H_s) \nabla g\} dS \quad (1b)$$

$$n_s = (0, 0, 1) \quad (2)$$

$$g = \frac{e^{-jkr}}{4\pi r} \quad (3a)$$

$$r = \sqrt{(x-x')^2 + (y-y')^2 + (z-z')^2} \quad (3b)$$

where  $g$  is the three-dimensional scalar Green function in free space, and  $r$  denotes the distance between a point  $(x, y, z)$  on  $S$  and an

observation point  $(x', y', z')$ . In the case of  $TE_{0n}$  mode incidence, the field vectors  $\mathbf{E}_S$  and  $\mathbf{H}_S$  on  $S$  are described in the cylindrical coordinates  $(\rho, \phi, z)$  by the following equations,

$$\left. \begin{aligned} E_\rho &= 0 & H_\rho &= -\frac{j\beta}{k_c} J_0'(k_c \rho) \\ E_\phi &= \frac{j\omega\mu}{k_c} J_0'(k_c \rho) & H_\phi &= 0 \\ E_z &= 0 & H_z &= J_0(k_c \rho) \end{aligned} \right\}, \quad (4a)$$

$$k_c = \frac{\chi_{0n}'}{a}, \quad \beta = \sqrt{k^2 - k_c^2}, \quad (4b)$$

where  $\chi'_{0n}$  is the  $n$ -th root of  $J_0'(x) = 0$ , and  $k$  is the wavenumber  $2\pi/\lambda$ .

Equations (1a) and (1b) are based on the Huygens-Fresnel principle, and the obtained field is the direct radiation field into free space, in other words, the field without the visor section.

The direct radiation field illuminates the visor surface,  $S_V$ , and generates the first reflection field  $\mathbf{E}_{r1}$  and  $\mathbf{H}_{r1}$  which satisfy the following boundary conditions on conductor.

$$\begin{aligned} \mathbf{n}_v \cdot \mathbf{E}_{r1} &= \mathbf{n}_v \cdot \mathbf{E}_i, & \mathbf{n}_v \times \mathbf{E}_{r1} &= -\mathbf{n}_v \times \mathbf{E}_i, \\ \mathbf{n}_v \cdot \mathbf{H}_{r1} &= -\mathbf{n}_v \cdot \mathbf{H}_i, & \mathbf{n}_v \times \mathbf{H}_{r1} &= \mathbf{n}_v \times \mathbf{H}_i \quad (\text{on } S_V). \end{aligned} \quad (5)$$

The first reflection field at an observation point is then calculated with the following equations, which are obtained by substituting Eqs. (5) into the Huygens-Fresnel formulae.

$$\mathbf{E}_{r1} = \int_{S_V} \{-j\omega\mu(\mathbf{n}_v \times \mathbf{H}_i) \mathbf{g} - (\mathbf{n}_v \times \mathbf{E}_i) \times \nabla \mathbf{g} + (\mathbf{n}_v \cdot \mathbf{E}_i) \nabla \mathbf{g}\} dS \quad (6a)$$

$$\mathbf{H}_{r1} = \int_{S_V} \{-j\omega\epsilon(\mathbf{n}_v \times \mathbf{E}_i) \mathbf{g} + (\mathbf{n}_v \times \mathbf{H}_i) \times \nabla \mathbf{g} - (\mathbf{n}_v \cdot \mathbf{H}_i) \nabla \mathbf{g}\} dS. \quad (6b)$$

The first reflection field gives rise to the second reflection field in the same process on the visor, viz,

$$E_{r2} = \int_{S_v} \{-j\omega\mu(\mathbf{n}_v \times \mathbf{H}_{r1})\mathbf{g} - (\mathbf{n}_v \times \mathbf{E}_{r1}) \times \nabla \mathbf{g} + (\mathbf{n}_v \cdot \mathbf{E}_{r1}) \nabla \mathbf{g}\} dS \quad (7a)$$

$$H_{r2} = \int_{S_v} \{-j\omega\epsilon(\mathbf{n}_v \times \mathbf{E}_{r1})\mathbf{g} + (\mathbf{n}_v \times \mathbf{H}_{r1}) \times \nabla \mathbf{g} - (\mathbf{n}_v \cdot \mathbf{H}_{r1}) \nabla \mathbf{g}\} dS \quad (7b)$$

Much higher-order reflections can be calculated in the same procedure. But we assume that the diameter of the waveguide is enough larger than the wavelength, and the structure of the visor is open, so that the higher-order reflection field is sufficiently small. Therefore we will neglect reflection higher than second order. The total field is then approximated by superposition of direct radiation, first and second reflection fields,

$$\mathbf{E} \approx \mathbf{E}_i + \mathbf{E}_{r1} + \mathbf{E}_{r2}, \quad \mathbf{H} \approx \mathbf{H}_i + \mathbf{H}_{r1} + \mathbf{H}_{r2} \quad (8)$$

In order to simplify the calculation of total radiation field, we will introduce a virtual surface  $S_A + S_B$  as shown in Fig. 2. Once the field on the virtual surface is obtained, radiation field at any point can be calculated with the following integrations, without estimating respectively the direct radiation and the reflection field.

$$\mathbf{E} = \int_{S_A + S_B} \{-j\omega\mu(\mathbf{n} \times \mathbf{H})\mathbf{g} + (\mathbf{n} \times \mathbf{E}) \times \nabla \mathbf{g} + (\mathbf{n} \cdot \mathbf{E}) \nabla \mathbf{g}\} dS \quad (9a)$$

$$\mathbf{H} = \int_{S_A + S_B} \{j\omega\epsilon(\mathbf{n} \times \mathbf{E})\mathbf{g} + (\mathbf{n} \times \mathbf{H}) \times \nabla \mathbf{g} + (\mathbf{n} \cdot \mathbf{H}) \nabla \mathbf{g}\} dS \quad (9b)$$

where  $\mathbf{n}$  denotes the outward unit normal vector on  $S_A$  or  $S_B$ .

As for an obliquely cut waveguide feed shown in Fig. 1(b), one can calculate the radiation from it with the same procedure, having only to change the shape of the visor section  $S_v$ .

### 3. COMPARISON OF THE PRESENT METHOD AND OTHER METHODS

Some analytical methods, such as the aperture-field method and the current-distribution method,<sup>6)</sup> are generally used to calculate

radiation characteristics of reflector antennas.

The present method may be regarded as a variety of the aperture-field method. The integral equations (9a) and (9b) to calculate radiation from the virtual surface are, in fact, the same as those in the aperture-field method. But the field distribution on the virtual surface is calculated on the basis of Huygens-Fresnel principle in the present method. On the other hand, the field distribution used in the aperture-field method is obtained through the geometrical-optics approximation, which is valid only if the aperture, or the reflector, is far enough from the source. In the present case, the source is the aperture  $S$  of an uniform waveguide section, and the reflector is the visor section, being close to each other. We should, then, consider the radiation and reflection from the feed waveguide to the aperture on the basis of Huygens-Fresnel principle.

As for the current-distribution method, radiation field is represented by an integration of current distribution on a reflector. It is generally difficult to obtain the distribution rigorously. Usually the current distribution is approximated by  $I = 2n \times H_1$ , where  $H_1$  is incident magnetic field and  $n$  is a unit normal vector on a reflector surface. Assuming that the size of the reflector and the radius of curvature of it are large enough compared with the wavelength, that approximation gives good results in calculation of the main lobe. But the assumption is not in the present case, and hence we should describe radiation using not only incident magnetic field but also incident electric field.

In these two method the geometrical-optics approximation is usually used to obtain source field, in which approximation shadow section of a reflector, not illuminated by geometrical rays, causes no difference on radiation characteristics. In the present problem, however, the shadow section on the visor has a great influence on the radiation field, especially on side-lobe level, which will be mentioned in the following section. The present method does not employ the geometrical-optics approximation, so that we can take the shape of the visor section into consideration.

#### 4. NUMERICAL RESULTS AND COMPARISON WITH EXPERIMENTAL RESULTS

Calculated and radiated patterns from feed waveguides are shown in Fig. 4, 5 and 6: operating frequency is 35.5 GHz ( $\lambda = 8.445$  mm), radius  $a$  of each waveguide is 16 mm ( $d = 32$  mm =  $3.79 \lambda$ ), and  $TE_{01}$  mode incident.

When we consider the propagation and radiation of circular  $TE_{0n}$  mode on the basis of the geometrical optics, the mode field is represented by superposition of quasi-optical rays, or local plane waves. Each of the rays propagates at a constant angle  $\alpha$  with the waveguide axis, where  $\alpha = \sin^{-1}(k_c/k)$ .<sup>1,3)</sup> In the present cases  $\alpha$  is equal to 18.8 degrees.

The visor section of a feed waveguide reflects the rays and forms a main lobe in the direction of  $\theta = -\alpha$ . The length  $L_0$  of the visor is determined by the geometrical optics,<sup>1,3)</sup>

$$L_0 = 2a \cot \alpha \quad (10)$$

In the present cases, the length is equal to 94.1 mm.

Fig. 4 shows the radiation from an oblique-cut feed with a visor of length  $L$  being 94.7 mm. Fig. 5 and Fig. 6 show that from stair-cut

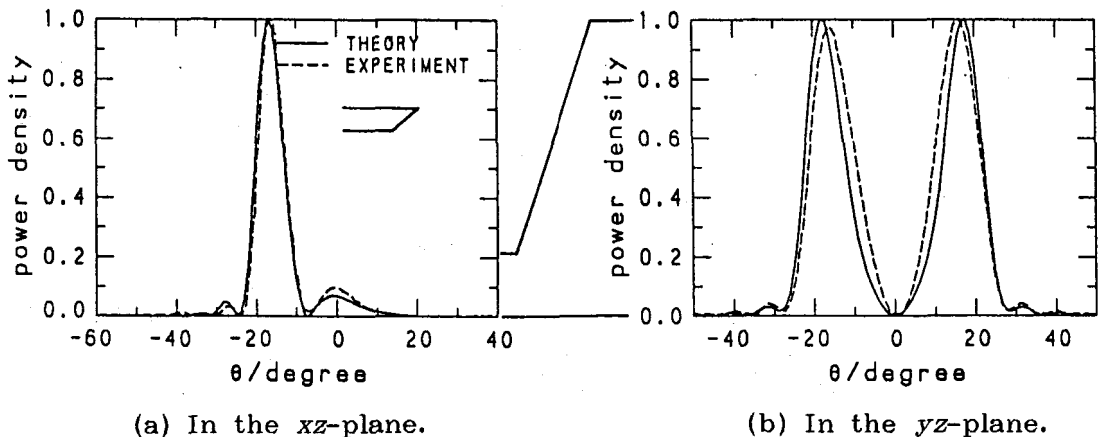


Fig. 4 Radiation pattern of an oblique-cut feed :  $L = 94.7$  mm,  $d = 32.0$  mm,  $f = 35.5$  GHz,  $TE_{01}$  mode incidence,  $\alpha = 18.8$  degree,  $\theta$ -polarized field.



feeds, where the length of the visors is 94.7 mm and 144.7 mm respectively. The distance between a feed and an observation point is fixed to be 500 mm. Solid curves denote the calculated radiation patterns and dashed curves, the measured ones. In each figure (a) shows normalized power density of main polarization,  $\theta$ -polarized, field in the  $xz$ -plane which is a symmetric plane of the visor, and (b) shows that in the  $yz$ -plane.

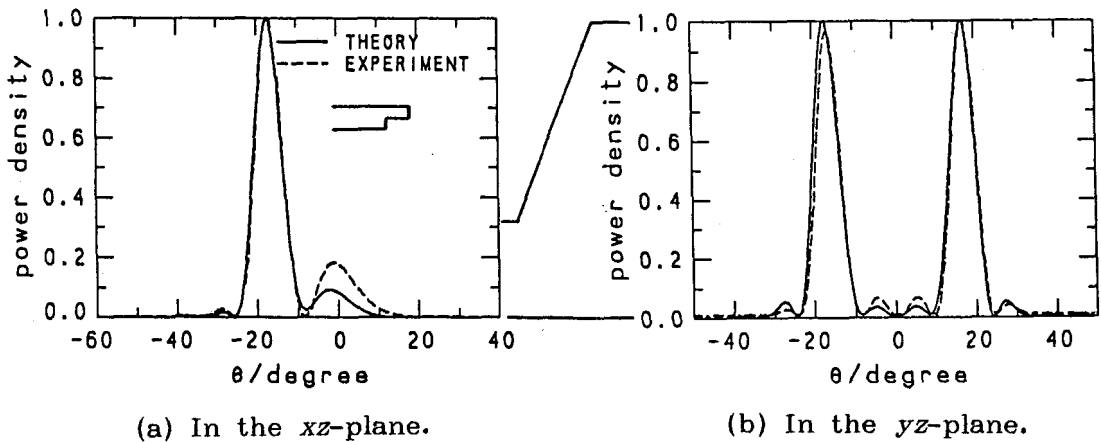


Fig. 5 Radiation pattern of an stair-cut feed :  $L = 94.7$  mm,  $d=32.0$  mm,  $f= 35.5$  GHz,  $TE_{01}$  mode incidence,  $\alpha=18.8$  degree,  $\theta$ -polarized field.

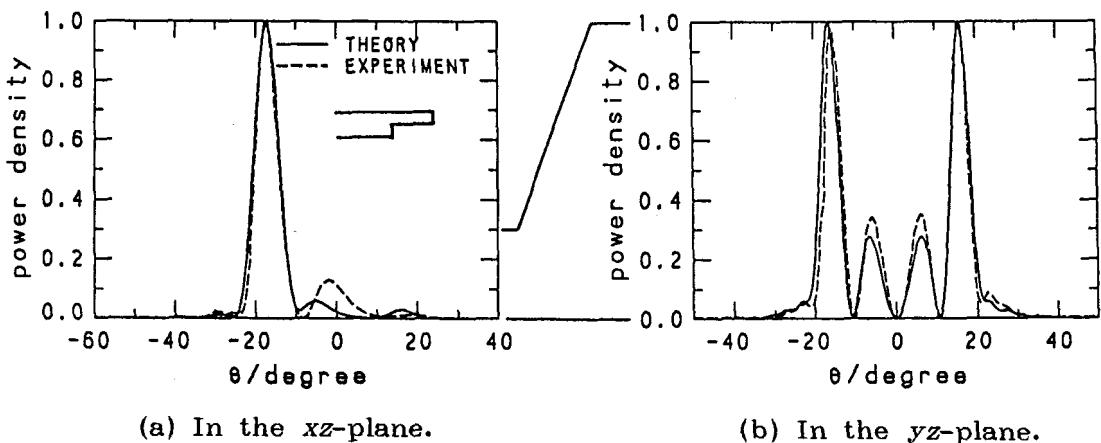
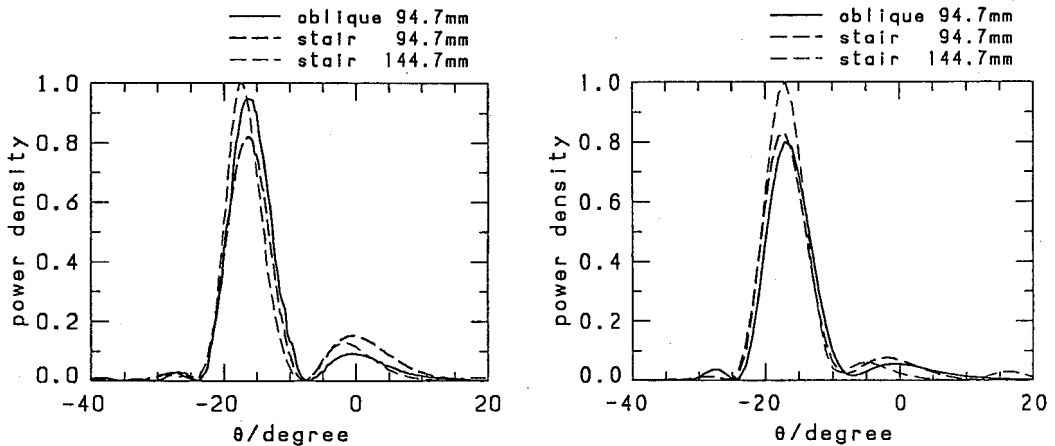


Fig. 6 Radiation pattern of an stair-cut feed :  $L = 144.7$  mm,  $d=32.0$  mm,  $f= 35.5$  GHz,  $TE_{01}$  mode incidence,  $\alpha=18.8$  degree,  $\theta$ -polarized field.

Calculated ratio of the peak level of the main lobe in (a) to the peak in (b) is 0.23 for Fig. 4, 0.33 for Fig. 5, and 0.30 for Fig. 6 respectively. With regard to the main lobe the measured results agree well with the calculated results.

As for stair-cut feeds, disagreement between measured and calculated results is noticeable in the direction of waveguide axis. The disagreement may be caused by diffraction field radiated from edge current, which is induced on the semicircle at the end of the visor. The edge is parallel with the incident electric field, so that the radiation by the edge current is in phase and emphasized in the direction of waveguide axis. The strength of the diffraction field is proportional to the intensity of the incident field at the edge. Using a long visor, the side-lobe level is reduced as shown in Fig. 6. As for the obliquely-cut feed, diffraction at the edge of the visor is less than that at a stair-cut feed because of gradual change of the shape and obliqueness of the edge.

Fig. 7 (a) represents the comparison of experimental field strength, and Fig. 7 (b) shows the calculated counterpart. In comparison of the two stair-cut feeds, good agreement is obtained in relative level of the main lobes. In order to obtain much better



(a) Experimental patterns.

(b) Theoretical patterns.

Fig. 7 Comparison of radiation patterns in the  $xz$ -plane.

agreement even on side lobes, we should estimate the above-mentioned edge current. As for the oblique-cut feed, the main-lobe level is lower than that of the stair-cut feed, that is explained by the fact that the beam width in the horizontal direction is wider than that of the stair-cut feed as shown in Fig. 4(b).

## 5. CONCLUSIONS

Making use of the Huygens-Fresnel formulae, we obtained the radiation characteristics of primary-feed waveguides for  $TE_{0n}$  mode. In these types of waveguides, the shadow section on the visor has a great influence on the radiation field, especially on the level of the main lobe and side lobes. The agreement between theoretical and experimental results was well for the oblique-cut feed. As for the stair-cut feed, disagreement was observed in the direction of the waveguide axis due to edge diffraction effect at the end of the visor section.

In order to obtain much better agreement between theoretical results and experimental results, we should estimate edge current at the end of the visor. The estimation is difficult when the distance between source and the edge is not far enough and the radius of curvature of the edge is not large enough compared with the wavelength, as is often the case with those feeds.

From the results of calculation and measurement, we can conclude that the length of the visor should be longer than that obtained by the geometrical optics, and the longer visor reduces the level of the side-lobe in the direction of the waveguide axis. In comparison of two types of feeds, an oblique-cut feed has lower side lobe, but the peak level of the main lobe is also lower because of its widespread radiation characteristics. Accordingly, the oblique-cut feed is suitable to the applications in which low side-lobe level is needed, and the stair-cut feed is suitable to those in which high efficiency of power transformation is required.

## ACKNOWLEDGMENTS

The author wishes to thank Professor M. Nakajima in Kyoto University for his kind guidance and fruitful discussions.

## References

- 1) S.N. Vlasov and I.M. Orlova : Radiophysics and Quantum Electronics  
17 (1975) 115-119.
- 2) Y. Akiyama, T. Yukawa, M. Nakajima and J. Ikenoue : IECE  
Technical Report, MW82-6 (1982).
- 3) O. Wada and M. Nakajima : Proc. 6th Joint Workshop on Electron  
Cyclotron Emission and Electron Cyclotron Resonance Heating,  
Oxford (1987) 369-376.
- 4) T. Saito *et al.* : Conf. Digest 9th Int. Conf. on Infrared and  
Millimeter waves (1984) 363-364.
- 5) R. Ainsworth *et al.* : Extended Synopses of 11th Int. Conf. on  
Plasma physics and Controlled Nuclear Fusion Research,  
IAEA-CN-47, F-III-2 (1986) 182-183.
- 6) S. Silver (editor) : Microwave Antenna Theory and Design  
(McGraw-Hill, New York, 1949) 137.